Investigating the role of NFAT transcription factors in acute lymphoblastic leukemia

by

Yuyin Wang

Bachelor of Science, University of Arizona, 2022

Submitted to the Graduate Faculty of the

School of Pharmacy in partial fulfillment

of the requirements for the degree of

Master of Science

University of Pittsburgh

2024

UNIVERSITY OF PITTSBURGH

SCHOOL OF PHARMACY

This thesis or dissertation was presented

by

Yuyin Wang

It was defended on

Select the Date

and approved by

Dr. Christian Fernandez, Associate Professor, Department of Pharmaceutical Sciences

Dr. Song Li, Professor, Department of Pharmaceutical Sciences

Dr. Robert Gibbs, Professor, Department of Pharmaceutical Sciences

Thesis Advisor: Dr. Christian Fernandez, Associate Professor, Department of Pharmaceutical Sciences

Investigating the role of NFAT transcription factors in acute lymphoblastic leukemia

Yuyin Wang, Bachelor of Science

University of Pittsburgh, 2024

Acute lymphoblastic leukemia (ALL) is one of the most common pediatric cancers originating in the bone marrow. Personalized therapy targeting specific high-risk ALL subtypes can significantly improve treatment outcomes. The nuclear factor of activated T cells (NFAT) can potentially be a therapeutic target in ALL. NFATs are transcription factors that play crucial roles in lymphocyte regulation and have been implicated in various cancers, including breast cancer, other leukemias, and so on. However, their roles in ALL remain unclear. We hypothesize that ALL cells have constitutively active NFATs, and inhibiting the transcriptional activity of NFATs can suppress the growth and proliferation of ALL. RNA-seq analysis of pediatric ALL patient samples identified various ALL subtypes with unfavorable prognosis and upregulated NFAT expression. Constitutive activation of NFAT in ALL cell lines was evaluated by a western blot of cytoplasmic and nuclear extract compared to normal human PBMCs (peripheral blood mononuclear cells). We show that pharmacological NFAT inhibition in ALL cell lines resulted in reduced cell proliferation, which correlated with the NFAT expression of the cells. ALL murine models were used to assess the translational potential of NFAT inhibition in vivo.

Table of Contents

Preface x

1.0 Introduction 1

1.1 ALL is cancer of the bone marrow 1

1.1.1 ALL is the most common cancer in children, and it is characterized by a large number of immature lymphocytes 1

1.1.2 Patients with unfavorable ALL subtypes may receive a higher dose of chemo drug or additional agent. 2

1.2 There are several different subtypes of pediatric ALL, some of which receive personalized therapy 3

1.2.1 ALL subtypes are determined by gene patterns and alterations 3

1.3 NFAT is a transcriptional factor that plays an important role in lymphocyte function 4

1.3.1 NFAT activation is based on the Ca2+-calcineurin-NFAT signaling pathway 4

1.3.2 NFAT proteins consist of two main regions that regulate their transcriptional activity 6

1.4 NFAT plays roles in the development of solid tumor and hematologic malignancies 6

1.5 Overview of thesis 8

2.0 ALL cells have constitutively active NFATs and inhibiting the transcriptional activity of NFATs can suppress the growth and proliferation of cancer cells 9

2.1 Methods and Materials 9

2.1.1 RNA-seq analysis of ALL patient samples 9

2.1.2 RNA extraction and RT-qPCR.....10

2.1.3 Western blotting assay.....11

2.1.4 siRNA knockdown.....12

2.1.5 Cell viability assay.....13

2.1.6 BCR-ABL mouse model development and engraftment monitoring.....14

2.1.7 Statistical analysis 15

2.2 Results..... 15

2.2.1 The expression of NFAT transcription factors is upregulated in ALL subtypes associated with poor prognosis 15

2.2.2 NFATs are dysregulated and constitutively active in ALL cell lines 22

2.2.3 Pharmacologic inhibition of NFATs attenuates the ALL cell proliferation in a dose-dependent method 25

2.2.4 Genetic inhibition of NFATC1 and NFATC2 can suppress the proliferation of ALL cells.....28

2.2.5 NFAT pharmacologic inhibition protects from ALL disease progression and leukemia burden.....31

3.0 Conclusions and future direction 34

List of Tables

Table 1: ALL patient samples from St. Jude Children's Research Hospital Pan-ALL dataset were classified based on subtypes and prognosis. 18

Table 2: Dysregulated NFATs of unfavorable prognosis subtypes with $p<0.05$ relative to favorable subtypes 21

Table 3: IC_{50} values of Cyclosporine A (CsA) and OR1011 on ALL cell lines. 27

List of Figures

Figure 1: Workflow of RNA-seq data from St. Jude Pan-ALL dataset analysis. 19

Figure 2: The fold change in NFATs expression of favorable prognosis subtypes relative to ETV6-RUNX ranged from 0.70 to 1.61. 20

Figure 3: NFATs are upregulated in ALL subtypes with unfavorable prognosis.. 21

Figure 4: NFATs are dysregulated and constitutively active in ALL cell lines. 24

Figure 5 Western blot of cytoplasmic and nuclear extract of NFATs in ALL cell lines and normal PBMCs. 24

Figure 6: Pharmacologic inhibition of NFATs attenuate ALL cell proliferation in a dose-dependent method 27

Figure 7: Genetic inhibition of NFATC1 and NFATC2 can suppress ALL cell proliferation. 30

Figure 8: NFAT pharmacologic inhibition attenuates ALL disease progression and leukemia burden 33

Acknowledge

Thanks to all.

1.0 Introduction

1.1 Acute Lymphoblastic Leukemia is a Cancer of the Bone Marrow

1.1.1 ALL is the most common cancer in children, and it is characterized by a large number of immature lymphocytes.

Acute lymphoblastic leukemia (ALL) is a type of cancer that affects the bone marrow, originating from immature lymphocytes such as precursor T and B cells [1]. It is characterized by a large number of immature lymphocytes and blockade of normal marrow cells. Around 6,000 patients are diagnosed by ALL annually in the USA, and an estimated 75% of them are younger than 20 years old [2]. Pediatric ALL is one of the most common cancers in children [3]. The basic symptoms of ALL include abnormal bleeding, fever, enlarged lymph nodes [3]. The potential causes are still unknown, but some evidence indicates the relationship between the ALL-disease progression and some risk factors like genetic mutation, severe radiation exposure, and so on [4, 5].

1.1.2 Patients with unfavorable ALL subtypes may additional or higher doses of chemotherapeutic agents.

ALL is always developing very rapidly over days or weeks, so the treatment should be given in time. The chemotherapy treatment of ALL can be divided into three phases: induction, consolidation and maintenance [6]. The goal of the treatment is to induce a complete hematologic remission (CHR) and prolong the remission duration. The backbone of pediatric ALL treatment includes glucocorticoids, vincristine, and asparaginase [7, 8]. Treatment is based on the prognosis, which is determined by several features, including age. The prognosis becomes worse with increasing age. The five-year relative survival rate of acute lymphoblastic leukemia patients is notably higher in children aged under 20 years old(80-90%) compared to adolescents (30-40%). The rate decreases to 20% for patients who are 40 or older [9]. High initial white blood cell count at diagnosis is also related to prognosis. Patients with WBC counts higher than 30,000/μL and 100,000/μL for B-ALL and T-ALL are determined as unfavorable prognosis [10].The subtypes, and the delayed response to the therapy are related to unfavorable prognosis as well[10]. Higher-risk patients who always have higher relapse rates may have to receive higher doses of the chemotherapeutic agents or have additional agents like cytarabine [11]. With the current chemotherapy treatment regimens, the 5-year survival rate of pediatric ALL patients is around 80-90% [12]. In addition to a high relapse rate, ALL patients also suffer from the severe side effects caused by chemotherapeutic agents so the novel target therapy is still needed.

1.2 There are several different subtypes of pediatric ALL, some of which receive personalized therapy.

1.2.1 ALL subtypes are determined by gene patterns and alterations.

ALL can be broadly divided into two types, B and T-cell lymphoblastic leukemia, based on immunophenotyping [1]. It can be further classified depending on the specific gene patterns and alterations. The identification of the subtypes is closely related to the disease evaluation and the treatment plan. Gene translocation is one of the most common abnormalities found in ALL, which occurs when a chromosome breaks into fragmented pieces and then attach to a different chromosome [13]. For example, the BCR-ABL1 subtype is caused by the gene fusion of BCR and ABL genes [14]. Numerical abnormalities are another type. The irregular change in the chromosome number is also associated with oncogenesis [4].

There are many different ALL subtypes, and some of them are associated with unfavorable prognosis such as BCR-ABL1 and BAR-ABL1 Like. Some of the ALL subtypes received "personalized" therapy, but many subtypes were treated using the same protocol or treatment. For example, BCR-ABL1 is determined by the gene fusion of the BCR gene and the ABL gene coding for a tyrosine kinase. So tyrosine kinase inhibitors (TKIs), including ponatinib, imatinib, and dasatinib, can be used to treat BCR-ABL1 ALL [15, 16]. BCR-ABL like has a significant genome overlap with BCR-ABL1. It lacks the gene fusion of BCR-ABL but contains various genome abnormalities that cause the abnormal activation of kinase signaling [17]. The treatment example of this subtype is the Janus kinase inhibitor, Ruxolitinib [18]. With the combination of target

therapy, the complete remission rate is significantly improved with minimal toxicity among BCR-ABL-positive patients [19]. However, few target therapies are available, and the outcome of other unfavorable prognosis ALL subtypes, such as T-ALL, should also be improved. A novel targeted therapy of ALL, especially for subtypes with unfavorable prognosis, is still needed.

1.3 NFAT is a transcriptional factor that plays an important role in lymphocyte function

1.3.1 NFAT activation is based on the Ca^{2+}-calcineurin-NFAT signaling pathway

The nuclear factor of activated T cells (NFAT) is a transcriptional factor that plays a critical role in the regulation of lymphocyte function, including activation and exhaustion. A typical immune response involves lymphocyte activation followed by rapid replications and subsequent differentiation of naïve lymphocytes to different effector lymphocytes, including T and B cells [20]. The two main types of effector T cells are helper T cells (CD4) and cytotoxic T cells (CD8). Helper T cells are divided into several subtypes, including T helper type I (TH1), TH2, TH17, T follicular helper (Tfh), and regulatory T (Treg) cells which are determined by the cytokine type they secreted, immune function they have, expression of transcription factors and chemokine receptors [21, 22]. TH1 helper cells can recruit the macrophage that can eliminate foreign substances and activate cytotoxic T cells. While TH2 helper cells activate B cells to secrete

antibodies [23]. TH17 secrete IL-17, IL-17F, IL-21 and IL-22 and recruite neutrophils and macrophages [24]. The primary function of Treg cells is maintaining self-tolerance to avoid auto-immune diseases [25]. Helper cells support the immune system based on the activation by TCR signaling [26]. Meanwhile, in contrast, after cytotoxic CD8 T cells recognize the specific antigen represented on the surface of the host cells, they program cell cytotoxicity to eliminate infected host cells by the secretion of toxins such as perforin and granzymes [27, 28]. Cytotoxic CD8 T cells also lead to apoptosis via Fas/FasL pathway [29]. T cell exhaustion is a type of T cell dysfunction commonly observed in cancers, which is caused by attenuated effector function that is closely related to the expression of multiple inhibitory receptors [30]. NFATs can regulate immune cell function via its activation by various cellular receptors, including immunoreceptor (TCR or BCR), receptor tyrosine kinases (RTKs), and G-protein-coupled receptor (GPCR), which are coupled to Ca^{2+} mobilization [31]. When immunoreceptors such as TCR, BCR, or receptor tyrosine kinases (RTKs), and G protein-coupled receptors (GPCRs) are triggered, a cascade of varying events converges at the activation of phosphatidylinositol-specific phospholipase C (PLC)-γ and β . PLC activation can then induce the hydrolysis of phosphatidylinositol-4,5-bisphosphate (PIP_2) to inositol-1,4,5-trisphosphate (IP_3). IP_3 binds to the IP3 receptors located in the endoplasmic reticulum (ER) and leads to the release of Ca^{2+} by depleting the Ca^{2+} stored in the ER. Elevated intracellular calcium levels from endoplasmic reticulum (ER) trigger the activation of calcium-release-activated calcium (CRAC) channel [32]. The stromal interaction molecule 1 (STIM1) and Orai1 are both critical to the function of the channel [32]. STIM1 can pass through the ER membrane, sense the depleted Ca^{2+} level, and communicate the Orai1 in the membrane to modify the Ca^{2+} level [32]. The binding of calcium to calmodulin induces the conformational change that leads to the activation of calmodulin [33]. The calmodulin binds to and stimulates the

phosphatase activity of calcineurin [33]. Calcineurin subsequently dephosphorylates and activates NFAT [31]. NFAT translocate from cytoplasm to nuclear after activation. In the nucleus, NFAT cooperates with different partners, such as AP-1, to regulate several types of genes, including those involved in the cell cycle regulation, growth, and activation of T cells which are closely related to the development of the immune response [34].

1.3.2 NFAT proteins consist of two main regions that regulate their transcriptional activity

There are four calcineurin-regulated family members in the NFAT family. NFATC1 and NFATC2 are highly expressed in lymphocytes, and NFATC3 is expressed in thymocytes. There are two main regions of NFAT protein: the NFAT-homology region (NHR) and the REL-homology region (RHR). NHR contains highly phosphorylated serine residue and binding site of calcineurin to regulate the transcriptional activation of NFAT. RHR includes a DNA-binding domain that has a binding point for NFAT's cooperator like AP-1 [35].

1.4 NFAT play roles in the development of solid tumors and hematologic malignancies

NFAT is also closely related to hematologic malignancies. NFAT are dysregulated, and they are involved in the regulation of genes that play important roles in cancer development. Recent research focusing on breast cancer investigates that NFATC1 is accumulated in the nucleus of triple-negative breast cancer, which is an aggressive type. NFAT regulates the expression of

COX-2, which is closely related to the cancer cell invasion [36]. Cyclooxygenase (COX) is an important enzyme that converts arachidonic acid into prostaglandins that play important roles in several body functions, including inflammation, healing, blood flow, and blood clot formation [37]. They can be pharmacologically inhibited by NS-398, Niflumic acid and NSAIDs (nonsteroidal anti-inflammatory drugs) like aspirin [36, 38, 39]. COX-2 abnormal activation is correlated with urokinase plasminogen activator (uPA), which is important in cancer invasion and metastasis [36]. In addition, both NFATC1 and NFATC2 inhibition suppress the tumor progression of triple-negative breast cancer [40, 41]. Except for breast cancer, NFATC1 is overexpressed and constitutively active in pancreatic cancer as well. NFAT regulates the expression of genes essential for pancreatic cancer cell proliferation, such as c-myc. Inhibition of NFATs can attenuate pancreatic cancer development [42, 43].

The dysregulation of NFAT is closely associated with both solid tumors and hematologic malignancies. NFATC1 is overexpressed and constitutively active in chronic lymphoblastic leukemia, and the inhibition of NFATC1 leads to a reduction in metabolic activity, which is a critical sign of cell proliferation [44]. NFATC1 is found to be overexpressed in subtypes of acute myeloid leukemia with unfavorable diagnosis [45], and the overexpression is related to resistance to sorafenib [45]. Both pharmacologic and genetic inhibition of NFAT can significantly increase the cancer cell apoptosis caused by sorafenib [45]. NFAT pharmacologic inhibition can also sensitize BCR-ABL-positive chronic myeloid leukemia cells to tyrosine kinase inhibitors, including imatinib and dasatinib [46]. However, NFAT function in acute lymphoblastic leukemia is still unknown.

1.5 Overview of the thesis

NFATs are important transcriptional factors that regulate lymphocyte function. It is overexpressed and constitutively active in several cancers including leukemias. NFAT can regulate the expression of oncogenes like COX-2, c-myc and so on in a cancer-specific manner. Inhibition of NFAT activation can decrease cancer cell proliferation, but few studies have investigated the role of NFATs in ALL, and there is still a need for novel target therapies for leukemias. We hypothesized that ALL cells have constitutively active NFATs, and inhibiting the transcriptional activity of NFATs can suppress the growth and proliferation of cancer cells. Our aims include the identification of ALL subtypes that overexpress NFATs, investigating the constitutive activation of NFATs in ALL cell lines, demonstrating that NFAT inhibition decreases the proliferation of ALL cell lines, and showing the antileukemic efficiency of NFAT inhibition using in vivo models of ALL.

2.0 ALL cells have constitutively active NFATs and inhibiting the transcriptional activity of NFATs can suppress the growth and proliferation of cancer cells

2.1 Methods and Materials

2.1.1 RNA-seq analysis of ALL patient samples

To assess the expression of NFAT transcription factors in acute lymphoblastic leukemia (ALL) patient samples, we used the St. Jude Pan-Acute Lymphoblastic Leukemia (PanALL) dataset [47] , which includes 735 ALL patient samples. ALL patients enrolled on ALL Total Therapy protocols Total XV (NCT00137111) [48], XVI (NCT00549848) [49], and XVII (NCT03117751) [50] were included in the Pan-Acute Lymphoblastic Leukemia dataset. We determined the prognosis based on the sample subtypes. We exclude the Hypodiploidy and NOS because they have significantly upregulated expression of NFATs compared to other favorable prognosis subtypes. Then, we exclude the unfavorable prognosis samples with a frequency lower than 4% because of the limited sample size. After that, we uploaded data to Partek Flow (Partek Inc., St. Louis, MO, USA) and normalized the gene counts by CPM (counts per million). We grouped favorable samples together because the fold change of NFATs expression in favorable subtypes relative to ETV6-RUNX is lower than 2. Then we filtered gene expression data of NFATC1, NFATC2, NFATC3 and NFATC4 out and exported to Graphpad Prism 10.1.2. The expression levels of different NFAT genes were analyzed by ANOVA with the post hoc analysis (Dunnett's multiple comparisons tests) to compare the difference between favorable prognosis samples to each of the unfavorable prognosis subtypes using GraphPad Prism 10.1.2. The normalized gene counts of NFATC1,

NFATC2, NFATC3, and NFATC4 of unfavorable prognosis subtypes were measured relative to favorable prognosis samples.

2.1.2 RNA extraction and RT-qPCR

Primers were diluted to 100 μM as stock. ALL cell lines were cultured in a 6-well plate in the concentration of $5x10^5$ cells/mL 18-24h before RNA extraction. Then, cells were washed with room-temperature PBS twice. 1 mL Trizol (Invitrogen, #446911) was added to each sample and resuspended well. Samples were left at room temperature for 5 minutes. After that 200 μL chloroform was added and the mixture is vortexed for 15 seconds. After incubation at room temperature for 3-5 minutes, samples were centrifuged at 12000 xg for 15 minutes at 4°C. The top layer of the gradient was taken and 1:1 ratio of 2-proponal was added carefully to avoid contamination. After vortex samples were left at room temperature for another 10 minutes. The they were centrifuged at 12000 xg for 10 minutes at 4°C. RNA extract from ALL cell lines should be washed by 75% ethanol twice and left at room temperature to dry for at least 40 minutes. 10 μl DEPC water was added to each sample and the concentration of the RNA samples were detected by Nanodrop.

Total RNA is converted to complementary DNA (cDNA) via reverse transcription. Primers were used to anneale the RNA strand and provide a starting point for transcriptase. Samples for reverse transcription were prepared by using kit (Fisher Scientific, #43-688-14) based on the calculation and be transcript to cDNA by PCR machine. cDNA of different samples were added to SYBR buffer and primer of NFATC1, NFATC2, NFATC3, NFATC4 and Gapdh. The SYBR

can attached to the double-strand of regions of DNA and release the fluorescent signal that can be detected by Quantstudio 6 Pro after spinning down the samples at 3000xg for 10 minutes. To test the knockdown efficiency of NFATC1 and NFATC2 on B-ALL, gene expression is normalized by TBP and 18s ribosomal RNA for REH and SUP-B15, respectively. Followings are the primers used: GAPDH (5'ACA TCG CTC AGA CAC CAT G 3') NFATC1(5'CTG TGC AAG CCG AAT TCT CTG G 3'); NFATC2(5' AAG AGC CAG CCC AAC ATG C 3'); NFATC3(5'CTG AGT CCC TGG ATT TAG GA 3'); NFATC4(5'AGC GTC ACC TCG TTG CTC TGC 3'); TBP (5'CTG GCC CAT AGT GAT CTT TGC 3'); 18s ribosomal RNA (5'GTA ACC CGT TGA ACC CCA TT 3').

2.1.3 Western blotting assay

Total protein was extracted from ALL cell lines by RIPA lysis and extraction buffer (Thermo Scientific, #89900) and Halt protease & Phosphatase Inhibitor Single-Use Cocktail (100x) (Thermo Scientific, #1861280) with the ratio of 99:1. To obtain cytoplasmic and nuclear extract separately, the Nuclear and Cytoplasmic Extraction kit (NE-PER, Pierce Biotechnology) was used. BCA Protein Assay Kit (Thermo Scientific, #23225) was conducted to determine the concentration of the protein sample. Based on the calculation, 20 µg of protein sample was added to each well on sodium dodecyl sulfate polyacrylamide gel electrophoresis (SDS-PAGE) using Mini-protein TGX Gls (BIO-RAD, #4561026). The gel was run in 1x Tris Buffer at 100 Voltage for 1-1.5 hours. After the complete separation, the protein was transferred to a methanol-activated PVDF membrane at 120V for 1.5-2 hours in 1x transfer buffer with 20% methanol at 4 °C. After the transfer, the membrane was blocked by 1x TBST buffer with 5% non-fat dry milk for 1 hour

at room temperature. Then the membrane was incubated with primary antibody overnight at 4 °C. The NFATC1 (Cell Signaling, #8032S), NFATC2 (Cell Signaling, #5861S), NFATC3 (Cell Signaling, #4998S), and NFATC4 (Cell Signaling, #2188S) antibodies were diluted 1:1000. Gapdh (Cell Signaling, #5174S) and Histone H3 (Cell Signaling, #3638S) antibodies were diluted 1:5000. The membrane was washed by the TBST buffer 10 minutes for three times and then the membranes were shaken with secondary antibody 1:10000 anti-rabbit IgG (Cell Signaling, #7074S) and anti-mouse IgG (Cell Signaling, #7076S) in 5% non-fat milk for 1 hour at room temperature. The secondary antibody can be conjugated to the horseradish peroxidase (HRP) enzyme. The membrane was washed again with 1x TBST buffer for 10 minutes three times and incubated with ECL Select Western Blotting Detection Reagent (Cytiva, #RPN2235) for 20 seconds, and HRP reacted with the substrate to provide an emitted signal that can be detected and exposed to film.

2.1.4 siRNA knockdown

Oligonucleotides of siRNA were used to knock down NFATC1 and NFATC2 in ALL cell lines. NFATC1 siRNA (sc-29412; Santa Cruz Biotechnology), NFATC2 siRNA (sc-36055; Santa Cruz Biotechnology), and control siRNA (sc-37007; Biotechnology) were introduced to ALL cell lines by Lipofectamine RNAiMAX (13-778-075; Invitrogen). The control siRNA consists of a scrambled sequence that does not target any degradation message. $5x10^6$ cells were cultured in each well in a 6-well plate. After incubating the diluted siRNA with the same amount of diluted Lipofectamine RNAiMAX for 5 minutes at room temperature, 205 μL of the mixture was added

dropwise to each well. Cell viability tests were conducted after incubation for 48 hours. RNA used for the knockdown efficiency test was extracted 24 hours after incubation.

2.1.5 Cell viability assay

Loucy, Reh and Molt-3 were cultured in RPMI 1640 (Thermo Fisher, # BW12-167-F12) with 10% non-HI FBS and 1% Pen-strep. Sup-b15 cells were cultured in IMDM with 20% HI-FBS and 0.1% 55mM 2-Mercaptoethanol (Thermo Fisher, 21985-023). ALL cell lines were plated in a 96-well plate with a concentration of $2x10^6$ cells/mL 18-24 hours before adding the inhibitors. ALL cells were treated with cyclosporine A or OR1011 (an investigational NFAT inhibitor synthesized by Organix, Inc) at concentrations of 0.1μM, 1 μM, 2.5 μM, 5 μM, 10 μM for 48 hours. Then 10μL yellow (substrate 3- (4,5-dimethylthiazol-2-yl)-2,5-diphenyltetrazolium bromide) MTT was added to each well, and the interaction lasted for about 2-3 hours. Active mitochondria can convert yellow MTT to purple formazon, which can be detected and measured. The activity of mitochondria works as the measurement of cell viability. 100μL mixture of 12mL 2-proponal and 40μL HCl was added to each well and incubate at 37°C for 20-30 minutes. Finally, the plate was read at the wavelength of 570 nm.

2.1.6 BCR-ABL mouse model development and disease progression measurement

To develop the BCR-ABL leukemia mouse model, the bone marrow cells extracted from ARF-null mice were transfected by the retroviral vectors encoding BCR-ABL gene fusion and luciferase. Then, $2x10^4$ BCR-ABL cells were injected into healthy C57BL/6 mice via tail intravenous injection. 10mg/kg of OR1011 was injected daily intraperitoneally into BCR-ABL mouse models. The mice were sacrificed upon 4% weight loss or upon development of hind limb paralysis. We investigated the significantly increased whole-body and bone marrow luminescence, spleen weight, and white blood cell count (WBC) compared to the group without any leukemia.

To measure the bioluminescence, 30mg D-Luciferase was dissolved in 2mL sterilized PBS and filtered by 0.22 mm filter. 150µL of luciferase was injected and waited for at least 10 minutes. After the anesthesia of mice by isoflurane, The bioluminescence imaging was made by IVIS Lumina XR, and mice were exposed to medium binning for auto time. ROI size with a width of 1.053 cm and a length of 3.156 cm. The signal is measured with the photon/sec/cm2/sr unit, which represents the number of photons/sec that leave the area of tissue and radiate to the sr angle. To measure the white blood cell count, blood was diluted by Turk's solution with a ratio of 1:10. The white blood cell number per µL can be counted and calculated. To acquire bone marrow cells, the bone marrow from hind limbs of mice was smashed through the cell stainer and washed with 5mL of Hank's Balance Salt Solution. After the lysis, the cells were spun down at 1500 rpm for 7 minutes at 4°C. Then, the cell pellet was resuspended in 1mL RBC lysis buffer and incubated for 5 minutes at room temperature. After the neutralization by adding 5mL of HI FBS, cells were centrifuged at 1500 rpm for 7 minutes at 4°C. To measure the bone marrow luciferase, 100µL cells and 100uL of Luciferase assay kit were added to 96-well and mixed well. After incubation at room

temperature for 10 minutes, the luminescence signaling from bone marrow cells extracted from the mice were measured and analyzed.

2.1.7 Statistical analysis

GraphPad Prism 10.1.2 was used to perform the statistical analysis of all data. The data were analyzed using a one-way analysis of variance (ANOVA) with Dunnett's multiple comparisons test (post hoc analysis) and t-test. Data were expressed as mean ± standard deviation (SD). P values less than or equal to 0.5 were considered as significant differences.

2.2 Results

2.2.1 The expression of NFAT transcription factors is upregulated in ALL subtypes associated with poor prognosis

Our goal is to demonstrate that the upregulation of NFATs plays an important role in the proliferation and progression of acute lymphoblastic leukemia. To determine whether NFAT transcription factors are dysregulated in ALL subtypes associated with poor prognosis, we analyzed RNA-sequencing (RNA-seq) data from the St. Jude Children's Research Hospital Pan-Acute Lymphoblastic Leukemia (Pan-ALL) dataset, which includes 735 patient samples (Figure 1) [51]. The leukemia samples were classified into 19 B-ALL and 6 T-ALL subtypes based on the

lymphoid ALL originated from. Sample prognosis was inferred based on the presence of specific gene or chromosome abnormalities. Overall, 28% of ALL samples included in the Pan-ALL dataset are associated with favorable prognosis, whereas 72% are considered ALL subtypes with unfavorable prognosis (Table 1). Specifically, favorable prognosis ALL subtypes included ETV6-RUNX1 (9.92%), DUX4-IGH (9.09%), ETV6-RUNX1 like (4.96%), ZNF384 rearrangement (2.69%), and NUTM1 rearrangement (1.24%) [52]. Comparing the expression levels of NFATC1, NFATC2, NFATC3, and NFATC4 in favorable prognosis subtypes to ETV6-RUNX1, we found that the fold change in expression levels relative to the ETV6-RUNX ranged from 0.70 to 1.61. (Figure 2A-D). Given the similar NFAT expression levels among the ALL subtypes with favorable prognosis, we grouped these ALL samples together for comparison to ALL subtypes associated with poor prognosis.

To identify ALL subtypes with upregulated NFAT expression that may benefit from NFAT inhibition, we focused our analysis on ALL subtypes with an incidence greater than 4% due to the limited size of our dataset. Therefore, we included BCR-ABL1 (5.79%), BCR-ABL Like (28.72%), iAMP21 (9.30%), PAX5 alteration (19.74%), MEF2D (4.55%), Hypodiploidy (5.17%) and T-ALL (7.02%) (>4%) leukemia subtypes in our analysis. We normalized the gene counts to counts per million (CPM) using Partek flow. To evaluate variations in mean NFATC1-4 expression across different ALL subtypes, we performed an ANOVA with post hoc analysis (Dunnett's multiple comparison test) to compare group means (Figure 1). Our results showed statistically significant variations in the expression of NFATC1, NFATC2, NFATC3, and NFATC4 ($P < 0.05$, Figure 3A-D), indicating NFAT dysregulation across the various leukemia subtypes analyzed. Based on these results, we subsequently performed post hoc analysis to identify

which ALL subtypes differed relative to ALL subtypes that are associated with favorable prognosis. We found that NFATC1 expression levels were upregulated in BCR-ABL Like, PAX5 alteration, Hypodiploid and MEF2D ALL subtypes relative to ALL subtypes with favorable prognosis(Figure 3A, Table 2). For NFATC2, its expression levels were significantly upregulated in all unfavorable subtypes except for subtypes with PAX5 alterations or hypodiploid ALL (Figure 2B, Table 2). Only iAMP21 and hypodiploid and MEF2D ALL subtypes had significantly upregulated NFATC3 expression (Figure 3C, Table 2), while NFATC4 expression was upregulated only in ALL subtypes with PAX5 alterations and MEF2D, relative to leukmeias with favorable subtypes (Figure 3D, Table 2). Based on RNA-seq analysis results, we conclude that several ALL subtypes associated with unfavorable prognosis have increased expression NFATs compared with favorable prognosis ALL, including leukemias harboring the BCR-ABL translocation. To investigate the biology significance of the results, we will test the constitutive activation of NFATs and conduct the inhibition of NFAT by using the patient samples.

Table 1: ALL patient samples from St. Jude Children's Research Hospital Pan-ALL dataset were classified based on subtypes and prognosis.

B-ALL		
Subtypes	Frequency %	Prognosis
ETV6-RUNX1	9.92	Favorable
ETV6-RUNX1 Like	4.96	Favorable
NUTM	1.24	Favorable
ZNF384	2.69	Favorable
DUX4-IGH	9.09	Favorable
PAX5	10.74	Unfavorable
MEF2D	4.55	Unfavorable
iAMP21	9.30	Unfavorable
Hypodiploidy	5.17	Unfavorable
BCR-ABL1	5.79	Unfavorable
BCR-ABL1 Like	28.72	Unfavorable
TOTAL B-ALL		
Prognosis	Frequency %	
Favorable	27.89	
Unfavorable	64.27	
B-ALL Total	92.15	
T-ALL		
Subtypes	Frequency %	
TLX3	0.92	Unfavorable
HOXA	1.66	Unfavorable
TAL1	0.37	Unfavorable
NOS	3.33	Unfavorable
SET-NUP14	0.37	Unfavorable
BCL-11B	0.37	Unfavorable
TOTAL T-ALL		
Prognosis	Frequency %	
Favorable	0.00	
Unfavorable	7.02	
T-ALL Total	7.02	
TOTAL ALL		
Prognosis	Frequency %	
Favorable	27.89	
Unfavorable	72.11	
ALL Total	100.00	

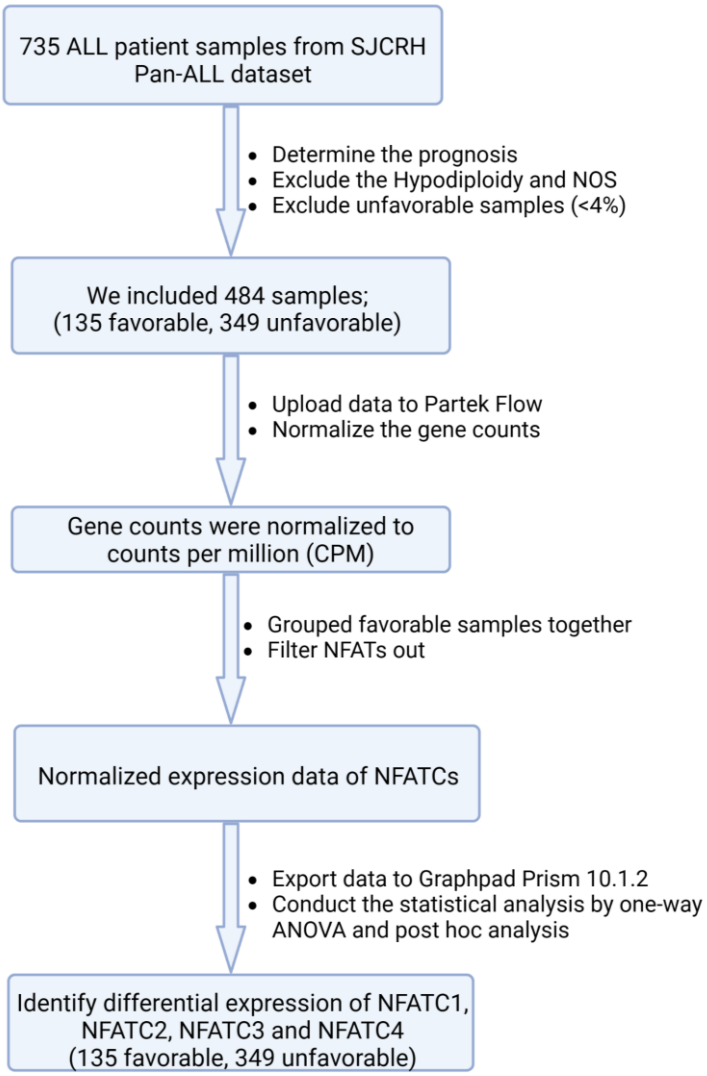

Figure 1: Workflow of RNA-seq data from St. Jude Pan-ALL dataset analysis.

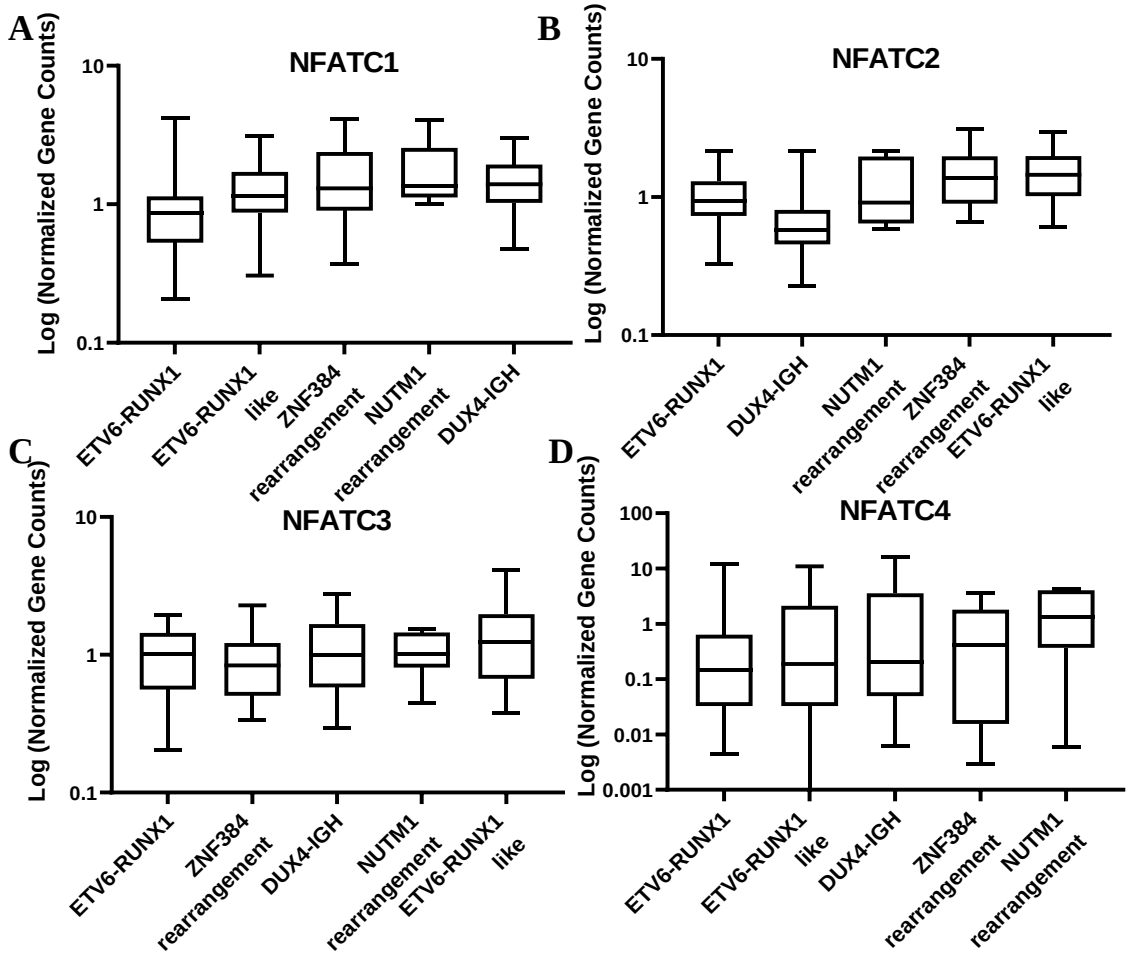

Figure 2: The fold change in NFATs expression of favorable prognosis subtypes relative to ETV6-RUNX ranged from 0.70 to 1.61.

(A), (B), (C), (D) Comparison of NFATC1, NFATC2, NFATC3 and NFATC4 expression levels in favorable prognosis subtypes relative to ETV6-RUNX.

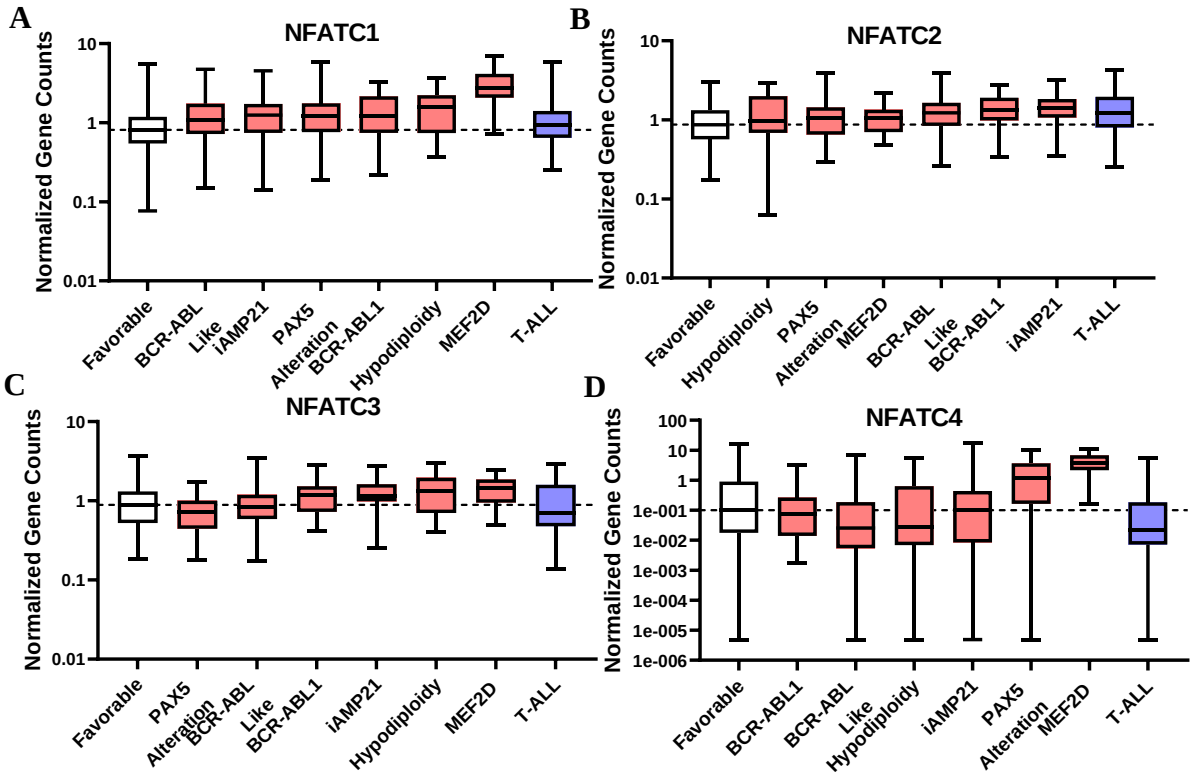

Figure 3: NFATs are upregulated in ALL subtypes with unfavorable prognosis. (A), (B), (C), (D) Comparison of NFATC1, NFATC2, NFATC3, and NFATC4 expression levels in ALL subtypes unfavorable prognosis (>4%) relative to favorable prognosis samples.

Table 2: Dysregulated NFATs of unfavorable prognosis subtypes with p<0.05 relative to favorable subtypes

ALL Subtypes	Frequency %	Dysregulated NFATs
BCR-ABL Like	28.72	NFATC1, NFATC2
PAX5 Alteration	10.74	NFATC1, NFATC4
iAMP21	9.30	NFATC2, NFATC3
T-ALL	7.01	NFATC2
BCR-ABL1	5.79	NFATC2
Hypodiploidy	5.17	NFATC1, NFATC3
MEF2D	4.55	NFATC1, NFATC2, NFATC3,NFATC4

2.2.2 NFATs are dysregulated and constitutively active in ALL cell lines.

Since we found that NFATs are dysregulated in the ALL subtypes with unfavorable prognosis, we next assessed the effect of pharmacological or genetic NFAT inhibition on ALL cell proliferaiton. We selected four cell lines for our analysis with variable expression of NFAT based on the CCLE (Cancer Cell Line Encyclopedia) database [53]. We included two B-ALL cell lines, REH and SUP-B15, and two T-ALL cell lines, MOLT-3 and LOUCY based on the CCLE database and availability. For B-ALL, the CCLE database indicates that SUP-B15 cells have higher NFAT expression levels compared to REH cells, whereas for the T-ALL, LOUCY cells have higher NFAT expression relative to MOLT-3. These cell lines can help us to assess whether NFATs are constitutively active in ALL cells and if there is a correlation between the NFAT expression level and cell proliferation inhibited pharmacologically or genetically. To confirm the expression level of NFAT in ALL cell lines, we assessed the mRNA and protein expression of the various cell lines by RT-qPCR and western blot. For the REH and SUP-B15 B-ALL cells, we confirmed that SUP-B15 cells have higher expression of NFATC1, NFATC2, NFATC3, and NFATC4 relative to REH cells (Figure 4A). Similarly, in T-ALL cells, the expression of NFATC1, NFATC2, NFATC3, and NFATC4 was higher in LOUCY cells compared to MOLT-3 cells (Figure 4A). Comparing our B and T-ALL cells, we found that T-ALL cell lines have higher NFATs mRNA expression relative to B-ALL cell lines (Figure 4A), indicating a potential differential response to NFAT inhibition between the different subtypes. The Western blotting results of the total protein expression level of NFATs show a similar trend (Figure 4B). SUP-B15 and LOUCY have higher mRNA expression level and total protein level of NFATs compared to REH and MOLT-3, respectively, and therefore they are potentially more sensitive to genetic or pharmacologic inhibition.

After the dephosphrlyation of NFAT by calcineurin, NFATs translocate from the cytoplasm to the nucleus where they can regulate the expression of target genes. Through mechanisms that are not well understood, constitutively active NFAT localized to the nucleus has been described in both solid tumors and some leukemias, such as acute myeloid leukemia, and regulates the expression of genes involved in cell growth [41, 42, 44]. To investigate the constitutive activation of NFATs in our ALL cell lines, we performed a western blot of cytoplasmic and nuclear NFAT protein levels to see whether NFATs are present in the nucleus without stimulation. Based on the comparison with normal human PBMCs, we show that NFATC1, NFATC2, and NFATC3 have higher expression levels in the nucleus than in the cytoplasm in all four cell lines, supporting that NFATs are constitutively active in our B- and T-ALLcell line models (Figure 5). Because NFATs regulate the transcription of several oncogenes, our results indicate that the constitutive activation of NFATs in our ALL cells potentially regulates their proliferation.

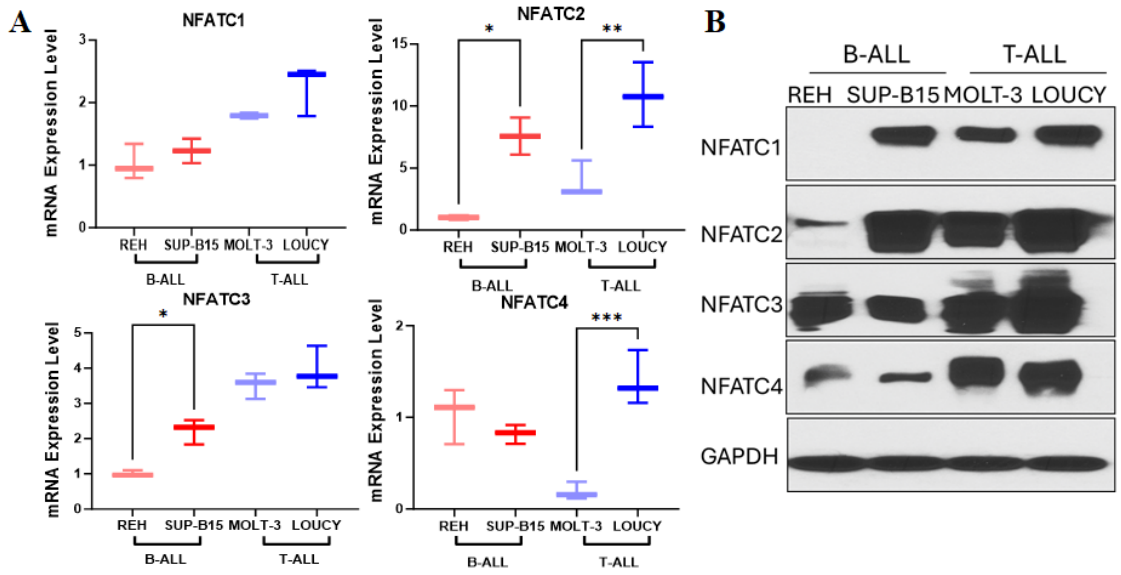

Figure 4: NFATs are dysregulated and constitutively active in ALL cell lines. (A) mRNA expression of NFATs in ALL cell lines. (B) Western blot of total protein of NFATs in ALL cell lines.

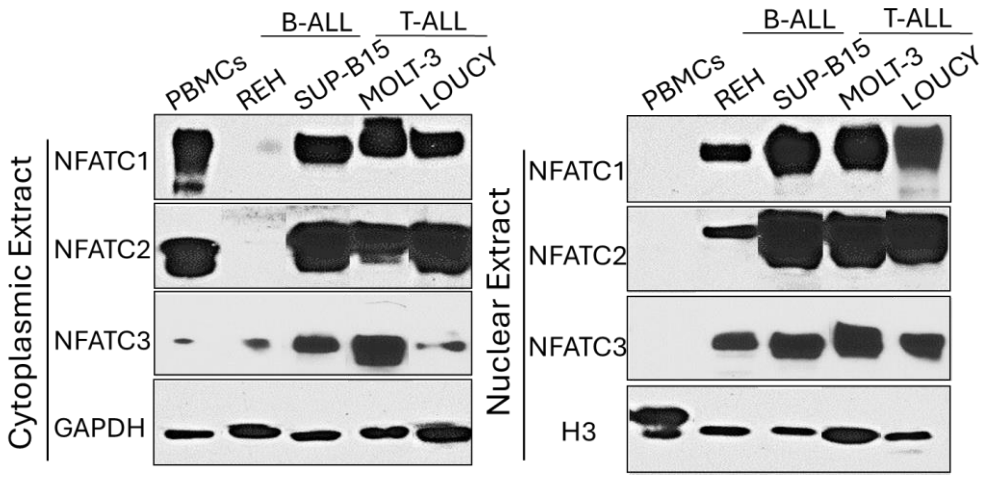

Figure 5 Western blot of cytoplasmic and nuclear extract of NFATs in ALL cell lines and normal PBMCs.

2.2.3 Pharmacologic inhibition of NFATs attenuates the ALL cell proliferation in a dose-dependent manner.

Two NFAT inhibitors with varying mechanisms of action were used in the study. The first is cyclosporine A (CsA). CsA is a well-known immunosuppression compound used to prevent the rejection of organs after transplantation surgery. CsA can block the phosphatase activity of calcineurin and thereby inhibit the translocation and activation of NFATs [54]. OR1011 is a novel small molecule compound discovered recently by our lab. It is a cannabinoid analog synthesized by Organix Inc. that was discovered through a large screen for NFAT inhibitors. It inhibits NFAT activation in a dose-dependent method with an IC_{50} value of 0.11 μM. It has suitable ADME properties, including solubility, microsomal stability, non-detected for kinase inhibition screen (468 kinases, 10 μM) and SafetyScreen 87 (10 μM). OR1011 also has acceptable PK properties like clearance, AUC, C_{max}, volume of distribution, and $T_{1/2}$. Through various studies, our lab has discovered that it does not interfere with calcineurin-mediated NFAT dephosphorylation or the translocation of NFATs from cytoplasm to nucleus, but rather attenuates the transcriptional activity of nuclear NFATs.

To determine the effect of pharmacologic inhibition of NFAT on ALL cell lines, we measured cell proliferation of ALL cell lines after treatment with CsA or OR1011 (0.1μM, 1 μM, 2.5 μM, 5 μM, 10 μM) for 48 hours. We chose these concentration points based on IC_{50} values (0.11 μM) of OR1011 on NFAT-luc reporter cells. We show that both CsA and OR1011 significantly inhibit the proliferation of B- and T-ALL cells in a dose-dependent manner (Figure 6A-D). For our B-ALL cells, we found that SUP-B15 cells (CsA IC_{50}=4.64μM; OR1011 IC_{50}=0.59μM) (Table 4) are more sensitive to CsA and OR1011 than REH cells (CsA

IC_{50}=6.83µM; OR1011 IC_{50}=3.67µM, Table 3, Figure 6A). For our T-ALL cell lines, we show that LOUCY cells are more sensitive to CsA (IC_{50}=2.58µM, Table 3) or OR1011 (IC_{50}=0.86µM) than MOLT-3 cells (CsA IC_{50}=5.18µM; OR1011 IC_{50}=1.47µM, Table 3, Figure 6B). Comparing B- and T-ALL cell lines, we found that T-ALL cells, which have higher NFAT mRNA and protein levels are more sensitive to CsA or OR1011 inhibition than B-ALL cells. Overall, we found that both CsA and OR1011 are both potent NFAT inhibitors that attenuate ALL cell proliferation in a concentration-dependent manner, and the cell lines with higher NFAT expression are more sensitive to NFAT inhibition. We also demonstrate that OR1011 is more potent at attenuating ALL cell proliferation than CsA, suggesting that its effect on nuclear NFAT may provide a superior approach for attenuating the transcriptional activity of NFAT.

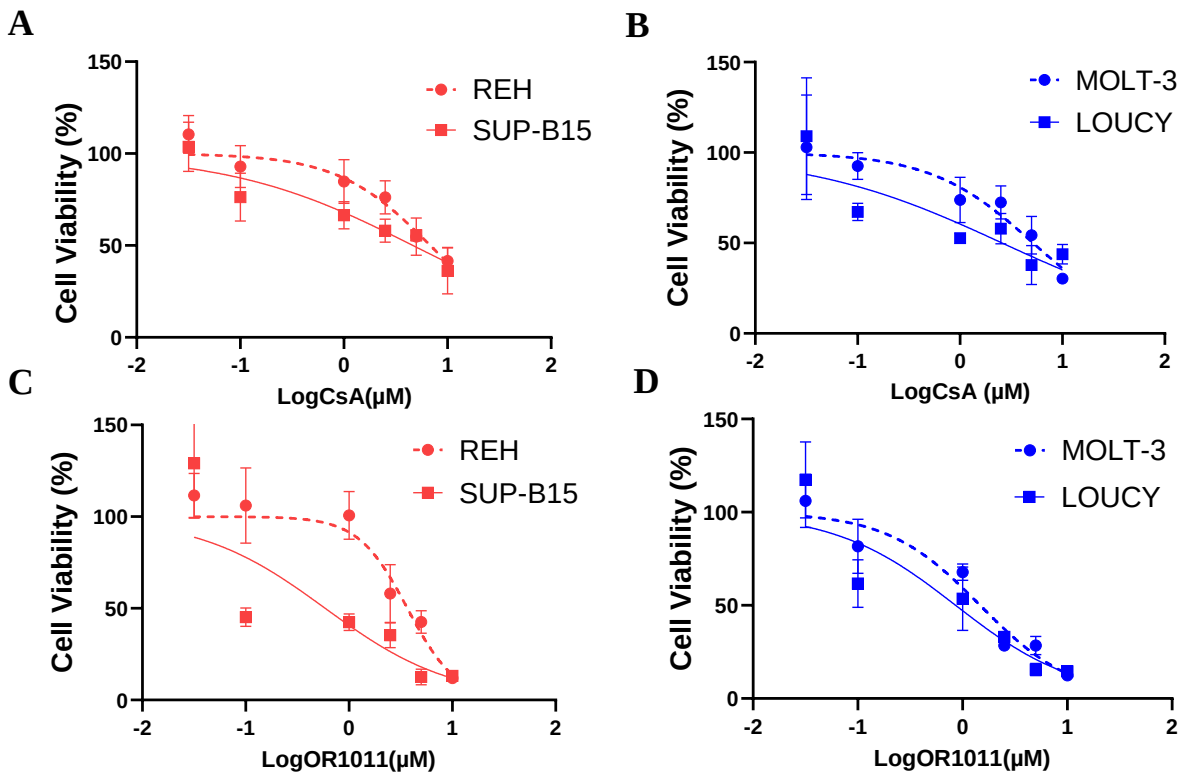

Figure 6: Pharmacologic inhibition of NFATs attenuate ALL cell proliferation in a dose-dependent method. (A), (B), (C), (D) % cell viability after ALL cell lines were incubated with CsA and OR1011 (0.1μM, 1 μM, 2.5 μM, 5 μM, 10 μM) for 48 hours.

Table 3: IC_{50} valus of Cyclosporine A (CsA) and OR1011 on ALL cell lines.

	B-ALL		T-ALL	
	REH	SUP-B15	MOLT-3	LOUCY
CsA IC_{50} (μM)	6.83	4.64	5.18	2.58
OR1011 IC_{50} (μM)	3.67	0.59	1.47	0.86

2.2.4 Genetic inhibition of NFATC1 and NFATC2 can suppress the proliferation of ALL cells

To verify the results of our pharmacological inhibition studies, we performed genetic NFAT inhibition studies using siRNA constructs targeting NFATC1 or NFATC2 on ALL cell lines. We specifically targeted NFATC1 and NFATC2 for our genetic inhibition studies because they are significantly upregulated in most ALL subtypes with unfavorable prognosis, constitutively active in ALL cell lines, differentially expressed in our high/low NFAT ALL cells, and are the two isotypes expressed at the highest levels in our four ALL cell lines. We assessed the efficiency of NFATC1 or NFATC2 knockdown on REH and SUP-B15 by RT-qPCR relative to scrambled siRNA controls. We found that NFATC1 siRNA attenuated the expression of NFATC1 in REH and SUP-B15 by 36% and 35%, respectively (Figure 7A-D). NFATC2 siRNA suppressed NFATC2 expression levels in REH and SUP-B15 by 42% and 56%, respectively (Figure 7A-D). However, we found that using this approach, there was no significant downregulation of NFAT levels in T-ALL, indicating that a more efficient knockdown method is needed to assess the effect of genetic NFAT inhibition in T-ALL.

Our study using NFATC1 or NFATC2 siRNA demonstrated that NFATC1 silencing suppressed the proliferation of REH and SUP-B15 by 29.8% and 39.0%, respectively, compared to the control group (Figure 7E-F). Using NFATC2 siRNA, we show that there is also a significant reduction of cell viability by 41.5% and 45.5% for REH and SUP-B15 (Figure 7E-F). Silencing of NFATC1 or NFATC2 on our T-ALL cell lines, MOLT-3, and LOUCY, led to no statistically significant reduction in cell proliferation (Figure 7G-H), consistent with our inability to potently inhibit NFAT expression using our siRNA constructs. We hypothesize that the higher NFAT

expression level in T-ALL relative to B-ALL contributes to our observations. Based on the results, we conclude that the genetic inhibition of NFATC1 or NFATC2 in ALL cells has a corresponding effect on cell proliferation. Nevertheless, there remains a need to evaluate the effect of more potent NFATC1 and NFATC2 knockdown on T-ALL cell growth.

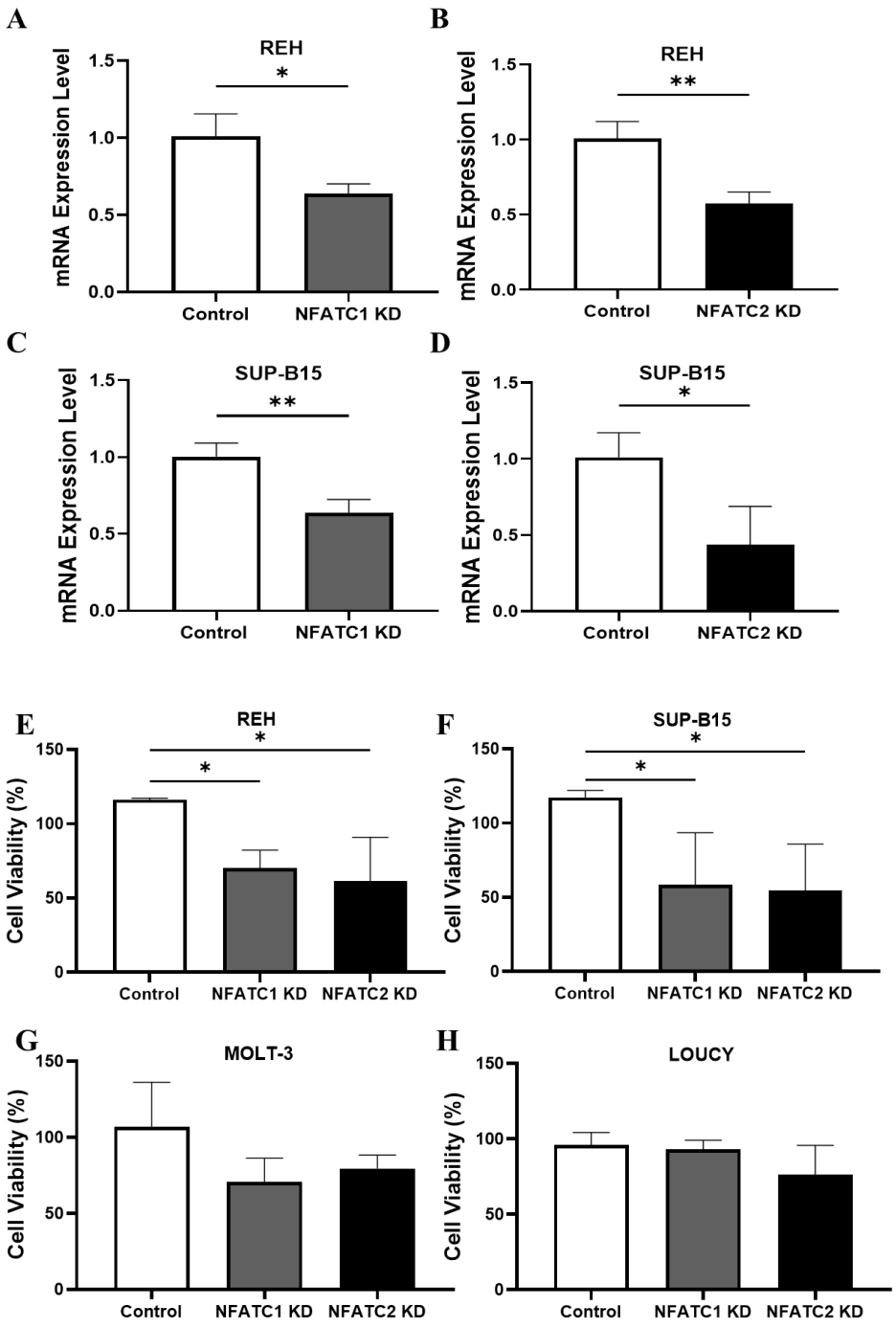

Figure 7: Genetic inhibition of NFATC1 and NFATC2 can suppress ALL cell proliferation. (A), (B), (C), (D) mRNA expression level of NFATC1 and NFATC2 after incubation of siRNA to test the knockdown efficiency on B-ALL. (E), (F), (G), (H) % Cell viability of REH, SUP-B15, MOLT-3 and LOUCY after incubation of Control siRNA, NFATC1 siRNA and NFATC2 siRNA.

2.2.5 NFAT pharmacologic inhibition protects from ALL disease progression and leukemia burden.

We found that both the pharmacologic and genetic inhibition of NFATs can inhibit ALL proliferation efficiently; our next step is to demonstrate the translational feasibility of NFATs inhibition by OR1011 and CsA using a mouse model of B-ALL driven by the BCR-ABL translocation [55]. Our murine model of BCR-ABL-induced ALL was used for this study due to the results of our clinical RNA-seq analysis, and because it is one of few syngenic models that is available and does not require immune suppression for in vivo analysis. To develop the BCR-ABL-induced leukemia murine models, bone marrow cells from ARF-null mice were transduced with the retroviral vector encoding the gene fusion of BCR-ABL and luciferase. After culturing and expanding the BCR-ABL positive bone marrow cells, $2x10^4$ cells were injected into healthy, non-condition mice to mimic human BCR-ABL positive ALL in immunocompetent C57BL/6 female mice (n=5 per treatment group) [55].

We first assessed the effect of CsA and OR1011 on the proliferation of BCR-ABL leukemia cells and found that both NFAT inhibitors attenuate the BCR-ABL ALL cell proliferation (Figure 8A), albeit OR1011 (IC_{50}=0.27μM) shows more potency in inhibiting the BCR-ABL cell proliferation compared to CsA (IC_{50}=3.35μM). ALL in vivo engraftment was monitored by bioluminescence imaging (BLI), where mice engrafted the leukemia cells 12 days after the cell administration, as indicated by the high BLI signal in mice inoculated with the leukemia cells (Figure 8B). Without treatment, this aggressive model of B-ALL leads to hind leg paralysis seventeen days after the cells are administrated, and mice that succumb to leukemia develop

elevated white blood cell (WBC) counts (Figure 8C), enlarged spleens (Figure 8D), and high bone marrow luciferase levels (Figure 8E), consistent with the development of severe ALL disease [56].

Having established our mouse model of aggressive B-ALL, we next assessed the effect of NFAT inhibition on this model using OR1011 and CsA. We first inoculated mice with BCR-ABL ALL cells, and seven days after the cell administration, we treated the mice with daily intraperitoneal 10mg/kg of OR1011 (n=5), 30mg/kg of CsA (n=5), or vehicle control. We monitored the leukemia engraftment on Day 12 of the protocol, and show that daily OR1011 or CsA treatment attenuates the in vivo whole-body BLI signal compared to vehicle control mice (Figure 8B, P value=0.0490 for OR1011 group; P value=0.0326 for CsA group). Furthermore, OR1011 or CsA treatment led to a 2-fold decrease in WBC counts (Figure8C, P value=0.0495 for OR1011 group; P value=0.0086 for CsA group) and decreased bone marrow luciferase levels (Figure 8E, p value=0.0016 for OR1011 group; p value<0.0001 for CsA group). However, OR1011 but not CsA treatment led to a significant reduction in spleen weight induced by the leukemia (Figure8D, P value=0.0203 for OR1011 group). While all vehicle control mice succumbed to ALL twenty-one days after the cell inoculation, OR1011 or CsA treatment extended survival by two and six days, respectively. (Figure 8F).

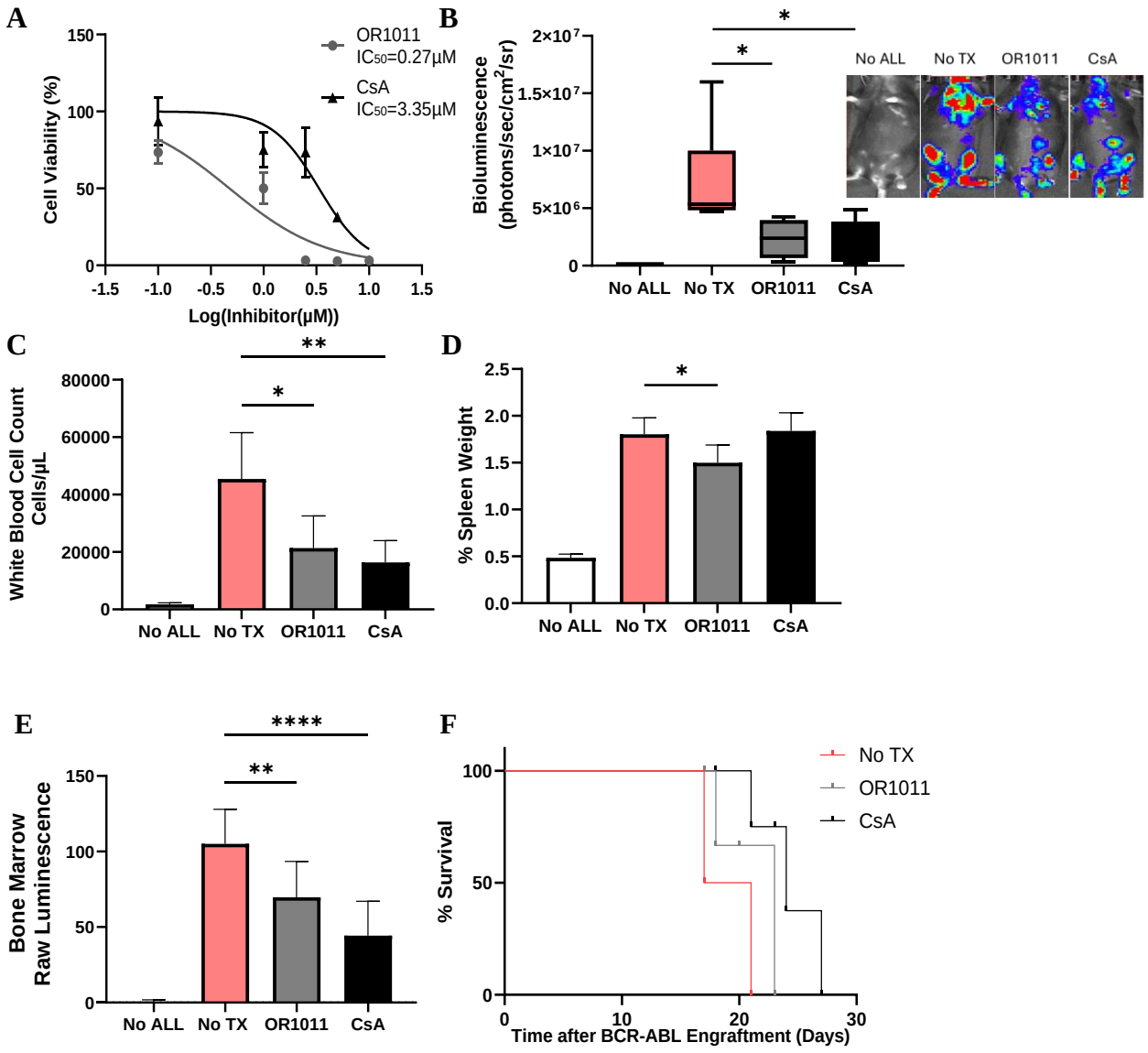

Figure 8: NFAT pharmacologic inhibition attenuates ALL disease progression and leukemia burden. (A) Cell viability (%) of BCR-ABL cells after incubation of OR1011 and CsA for 48 hours. (B) Whole-body bioluminescence of no ALL, no TX, 10 mg/kg OR1011, and 30 mg/kg CsA groups on Day 12. (C) White blood cell count (WBC) per µL of different groups after sacrifice. (D) %Spleen weight of control and treatment groups. (E) Bone marrow luciferase per 10000 cells for different groups (F) Survival rate of control and treatment groups.

3.0 Conclusions and Future Directions

To summarize, NFAT is an essential transcription factor that plays a critical role in several cancers, including leukemias [41, 42, 44]. However, the roles of NFAT in ALL are less understood. Based on the results of the RNA-seq analysis described in my thesis, NFAT expression level is higher in ALL subtypes with unfavorable prognosis compared to favorable ALL samples (Figure 3A-D). NFAT is constitutively active in ALL cell lines (Figure 5), and cell lines with higher NFAT expression levels are more sensitive to pharmacologic inhibition induced by CsA and OR1011 (Figure 6A-D). Genetic inhibition of NFATC1 and NFATC2 dramatically decrease the cell proliferation of B-ALL cell lines, indicating the critical role NFAT plays in ALL cell proliferation (Figure 7E-F). Both CsA (30mg/kg) and OR1011 (10mg/kg) treatments attenuated the progression of BCR-ABL leukemia disease and prolonged the survival of mice (Figure 8B-F). Taking together the results presented in my thesis, we propose that NFAT inhibition can potentially be an effective approach for treating ALL subtypes with unfavorable prognosis.

While our study has several limitations. Our siRNA approach was not effective enough to knockdown NFATC1 or NFATC2 in T-ALL cell lines. We will therefore develop a more efficient strategy, such as electroporation, to assess the effect of genetic NFAT inhibition on T-ALL cell proliferation and develop the cell lines with stable knock-down of NFATs including NFATC3 and NFATC4. We plan to inject these cells into immunocompromised mice to determine the impact of NFAT genetic inhibition on ALL disease progress in mice. In addition, our BCR-ABL mouse model is an aggressive model leading to death due to leukemia within twenty-one days of cell administration. To better assess the benefit of in vivo NFAT inhibition, we will modulate the aggressiveness of our model by attenuating the dose of BCR-ABL cells given to mice.

Furthermore, NFATs are found constitutively active in ALL cell lines and in other cancers such as breast cancer [40] and other leukemia [44]. However, the mechanism of constitutive activation in cancers is still unknown. One of the potential reasons is the mutation of crucial genes in calcineurin or notch1 signaling pathways that regulate the activation of NFATs [34, 57]. Therefore, a future objective is to use DNA sequencing data to examine the specific genes that are mutated in leukemias overexperessing NFAT, potentially resulting in the constitutive activation of NFATs in ALL. Moreover, while we demonstrate that NFATs play a critical role in ALL and that the inhibition of NFATs dramatically attenuated ALL proliferation, it is unknown which NFAT isoform is dominant or whether there is compensation by other NFATs. Our future directions will therefore assess the effect of genetic inhibition of one or several NFAT isoforms to test whether several NFAT isoforms regulate ALL proliferation. Based on our results of RNA-seq analysis of ALL patient samples and cell viability tests, our results suggest that ALL patients with unfavorable subtypes exhibit higher NFAT expression levels. These patients may potentially benefit from pharmacologic inhibition, as ALL cell lines with elevated NFAT expression tend to be more sensitive to NFAT inhibition. Nevertheless, clinical validation experiments are needed to validate whether NFAT overexpression is a suitable biomarker predicting response to NFAT inhibition. This study also lacks evidence regarding the mechanism through which NFAT inhibition attenuates ALL proliferation. NFAT is an important transcription factor that regulates the expression of several key genes in cancers, such as c-myc and cyclin D1 [42, 58]. By investigating the expression of the oncogenes that are regulated by NFAT, we will indicate the role NFAT plays in ALL development and the target genes that are involved in NFAT-driven ALL proliferation.

Another limitation is that we cannot currently pharmacologically inhibit specific NFAT isoforms, which may lead to potential safety concerns. CsA is a well-known immunosuppressive compound that inhibits the Ca^{2+}-calcineurin-NFAT signaling pathway used in this study. Aside from its effect on the immune system, it has several severe side effects based on clinical usage, including nephrotoxicity [59]. We therefore plan to assess the role of NFATs in CsA-mediated toxicities, including nephrotoxicity, to validate the safety of our approach.

Bibliography

1. Onciu, M., *Acute lymphoblastic leukemia.* Hematology/oncology clinics of North America, 2009. **23**(4): p. 655-674.
2. Malard, F. and M. Mohty, *Acute lymphoblastic leukaemia.* The Lancet, 2020. **395**(10230): p. 1146-1162.
3. Institute, N.C. *Childhood Acute Lymphoblastic Leukemia Treatment*. 2017 8 December 2017; Available from: https://www.cancer.gov/types/leukemia/hp/child-all-treatment-pdq#section_1.7.
4. Hunger, S.P. and C.G. Mullighan, *Acute lymphoblastic leukemia in children.* New England Journal of Medicine, 2015. **373**(16): p. 1541-1552.
5. Inaba, H., M. Greaves, and C.G. Mullighan, *Acute lymphoblastic leukaemia.* The Lancet, 2013. **381**(9881): p. 1943-1955.
6. Hussein, K.K., et al., *Treatment of acute lymphoblastic leukemia in adults with intensive induction, consolidation, and maintenance chemotherapy.* 1989.
7. Patel, A.A., et al., *Efficacy and tolerability of a modified pediatric‐inspired intensive regimen for acute lymphoblastic leukemia in older adults.* EJHaem, 2021. **2**(3): p. 413-420.
8. Raj, T.A.S., A.M. Smith, and A.S. Moore, *Vincristine sulfate liposomal injection for acute lymphoblastic leukemia.* International journal of nanomedicine, 2013: p. 4361-4369.
9. Geyer, M.B., et al., *Overall survival among older US adults with ALL remains low despite modest improvement since 1980: SEER analysis*. Blood, The Journal of the American Society of Hematology, 2017. **129**(13): p. 1878-1881.
10. *Acute lymphoblastic leukemia: Risk categories*. 2018 March 6th 2018 [cited 2018 March 6th]; Available from: https://www.aboutkidshealth.ca/article?contentid=2843&language=english#:~:text=High%2Drisk%20ALL,in%20the%20CSF%20(CNS%203).
11. Tadi., A.F.P., *National Library of Medicine: Cytarabine.* 2023.
12. Pui, C.-H. and W.E. Evans, *Acute lymphoblastic leukemia.* New England Journal of Medicine, 1998. **339**(9): p. 605-615.
13. Bell, D.W. *Translocation*. 2024 May 17 2024 May 17 2024]; Available from: https://www.genome.gov/genetics-glossary/Translocation.
14. Fine, B.M., et al., *Gene expression patterns associated with recurrent chromosomal translocations in acute lymphoblastic leukemia.* Blood, 2004. **103**(3): p. 1043-1049.
15. Hoelzer, D., *Personalized medicine in adult acute lymphoblastic leukemia.* Haematologica, 2015. **100**(7): p. 855.
16. Mei, L., et al., *Pharmacogenetics predictive of response and toxicity in acute lymphoblastic leukemia therapy.* Blood reviews, 2015. **29**(4): p. 243-249.
17. Tasian, S.K., M.L. Loh, and S.P. Hunger, *Philadelphia chromosome–like acute lymphoblastic leukemia.* Blood, The Journal of the American Society of Hematology, 2017. **130**(19): p. 2064-2072.

18. Chiaretti, S., M. Messina, and R. Foà, *BCR/ABL1–like acute lymphoblastic leukemia: How to diagnose and treat?* Cancer, 2019. **125**(2): p. 194-204.
19. Malagola, M., C. Papayannidis, and M. Baccarani, *Tyrosine kinase inhibitors in Ph+ acute lymphoblastic leukaemia: facts and perspectives.* Annals of hematology, 2016. **95**: p. 681-693.
20. Serfling, E., F. Berberich-Siebelt, and A. Avots, *NFAT in Lymphocytes: A Factor for All Events?* Science's STKE, 2007. **2007**(398): p. pe42-pe42.
21. Lee, G.R., *The Balance of Th17 versus Treg Cells in Autoimmunity.* Int J Mol Sci, 2018. **19**(3).
22. Nurieva, R.I. and Y. Chung, *Understanding the development and function of T follicular helper cells.* Cellular & Molecular Immunology, 2010. **7**(3): p. 190-197.
23. *Helper T-cells*. 2022; Available from: https://my.clevelandclinic.org/health/body/23193-helper-t-cells.
24. Martinez, G.J., et al., *Regulation and function of proinflammatory TH17 cells.* Ann N Y Acad Sci, 2008. **1143**: p. 188-211.
25. Corthay, A., *How do regulatory T cells work?* Scand J Immunol, 2009. **70**(4): p. 326-36.
26. Shah, K., et al., *T cell receptor (TCR) signaling in health and disease.* Signal Transduction and Targeted Therapy, 2021. **6**(1): p. 412.
27. Pennock, N.D., et al., *T cell responses: naive to memory and everything in between.* Advances in physiology education, 2013. **37**(4): p. 273-283.
28. Voskoboinik, I., J.C. Whisstock, and J.A. Trapani, *Perforin and granzymes: function, dysfunction and human pathology.* Nat Rev Immunol, 2015. **15**(6): p. 388-400.
29. Volpe, E., et al., *Fas-Fas Ligand: Checkpoint of T Cell Functions in Multiple Sclerosis.* Front Immunol, 2016. **7**: p. 382.
30. Thouenon, R. and G. Verdeil, *Tumor microenvironment squeezes out the juice from T cells.* Cell Res, 2024.
31. Hogan, P.G., et al., *Transcriptional regulation by calcium, calcineurin, and NFAT.* Genes & development, 2003. **17**(18): p. 2205-2232.
32. Berlansky, S., et al., *More Than Just Simple Interaction between STIM and Orai Proteins: CRAC Channel Function Enabled by a Network of Interactions with Regulatory Proteins.* Int J Mol Sci, 2021. **22**(1).
33. Park, H.S., et al., *Calcium-Calmodulin-Calcineurin Signaling: A Globally Conserved Virulence Cascade in Eukaryotic Microbial Pathogens.* Cell Host Microbe, 2019. **26**(4): p. 453-462.
34. Gao, R., et al., *The role of NFAT in the pathogenesis and targeted therapy of hematological malignancies.* European Journal of Pharmacology, 2022. **921**: p. 174889.
35. Macian, F., C. López-Rodríguez, and A. Rao, *Partners in transcription: NFAT and AP-1.* Oncogene, 2001. **20**(19): p. 2476-2489.
36. Singh, B., et al., *COX-2 overexpression increases motility and invasion of breast cancer cells.* International journal of oncology, 2005. **26**(5): p. 1393-1399.
37. *Prostaglandins.* 2022.
38. Larkins, T.L., et al., *Inhibition of cyclooxygenase-2 decreases breast cancer cell motility, invasion and matrix metalloproteinase expression.* BMC cancer, 2006. **6**: p. 1-12.
39. Cui, J. and J. Jia, *Natural COX-2 Inhibitors as Promising Anti-inflammatory Agents: An Update.* Curr Med Chem, 2021. **28**(18): p. 3622-3646.

40. Tran Quang, C., et al., *The calcineurin/NFAT pathway is activated in diagnostic breast cancer cases and is essential to survival and metastasis of mammary cancer cells.* Cell death & disease, 2015. **6**(2): p. e1658-e1658.
41. Yiu, G.K. and A. Toker, *NFAT induces breast cancer cell invasion by promoting the induction of cyclooxygenase-2.* Journal of Biological Chemistry, 2006. **281**(18): p. 12210-12217.
42. Buchholz, M., et al., *Overexpression of c-myc in pancreatic cancer caused by ectopic activation of NFATc1 and the Ca2+/calcineurin signaling pathway.* The EMBO journal, 2006. **25**(15): p. 3714-3724.
43. Ito, H., et al., *Prostaglandin E2 enhances pancreatic cancer invasiveness through an Ets-1-dependent induction of matrix metalloproteinase-2.* Cancer research, 2004. **64**(20): p. 7439-7446.
44. Le Roy, C., et al., *The degree of BCR and NFAT activation predicts clinical outcomes in chronic lymphocytic leukemia.* Blood, The Journal of the American Society of Hematology, 2012. **120**(2): p. 356-365.
45. Metzelder, S., et al., *NFATc1 as a therapeutic target in FLT3-ITD-positive AML.* Leukemia, 2015. **29**(7): p. 1470-1477.
46. Gregory, M.A., et al., *Wnt/Ca2+/NFAT signaling maintains survival of Ph+ leukemia cells upon inhibition of Bcr-Abl.* Cancer cell, 2010. **18**(1): p. 74-87.
47. Lee, S.H., et al., *Pharmacotypes across the genomic landscape of pediatric acute lymphoblastic leukemia and impact on treatment response.* Nature medicine, 2023. **29**(1): p. 170-179.
48. *Therapy for Newly Diagnosed Patients With Acute Lymphoblastic Leukemia*. 2020 2020-09-11 [cited 2020 2020-09-11]; Available from: https://clinicaltrials.gov/study/NCT00137111.
49. *Total Therapy Study XVI for Newly Diagnosed Patients With Acute Lymphoblastic Leukemia*. 2022 2022-08-23 [cited 2022 2022-08-23]; Available from: https://clinicaltrials.gov/study/NCT00549848.
50. *Total Therapy XVII for Newly Diagnosed Patients With Acute Lymphoblastic Leukemia and Lymphoma*. 2017 2024-03-05 [cited 2017 2017-04-18]; Available from: https://classic.clinicaltrials.gov/ct2/show/NCT03117751.
51. Holmfeldt, L., et al., *The genomic landscape of hypodiploid acute lymphoblastic leukemia.* Nature genetics, 2013. **45**(3): p. 242-252.
52. Network, N.C.C. *Acute Lymphoblastic Leukemia (Version 4.2023)*. February 05, 2024]; Available from: https://www.nccn.org/professionals/physician_gls/pdf/all.pdf.
53. *Broad-Novartis Cancer Cell Line Encyclopedia*.
54. Jørgensen, K.A., P. Koefoed‐Nielsen, and N. Karamperis, *Calcineurin phosphatase activity and immunosuppression. A review on the role of calcineurin phosphatase activity and the immunosuppressive effect of cyclosporin A and tacrolimus.* Scandinavian journal of immunology, 2003. **57**(2): p. 93-98.
55. Williams, R.T., M.F. Roussel, and C.J. Sherr, *Arf gene loss enhances oncogenicity and limits imatinib response in mouse models of Bcr-Abl-induced acute lymphoblastic leukemia.* Proceedings of the National Academy of Sciences, 2006. **103**(17): p. 6688-6693.
56. Boulos, N., et al., *Chemotherapeutic agents circumvent emergence of dasatinib-resistant BCR-ABL kinase mutations in a precise mouse model of Philadelphia chromosome–*

positive acute lymphoblastic leukemia. Blood, The Journal of the American Society of Hematology, 2011. **117**(13): p. 3585-3595.
57. Izon, D.J., et al., *Notch1 regulates maturation of CD4+ and CD8+ thymocytes by modulating TCR signal strength.* Immunity, 2001. **14**(3): p. 253-264.
58. Baksh, S., et al., *NFATc2-mediated repression of cyclin-dependent kinase 4 expression.* Molecular cell, 2002. **10**(5): p. 1071-1081.
59. Wu, Q., et al., *Mechanism of cyclosporine A nephrotoxicity: Oxidative stress, autophagy, and signalings.* Food and chemical toxicology, 2018. **118**: p. 889-907.